

POLYTECHNIC OF NAMIBIA



SCHOOL OF ENGINEERING (DEPARTMENT OF MECHANICAL ENGINEERING)

Development of a Sun Tracking System for a Small Solar Concentrator

**C. Mutaleni (B.Tech Student)
Isabel Bishi
Andrew Zulu
Dr. Swaminathan Rajaram
(Department of Mechanical Engineering)**

(Research project no: IRPC-POLY/2010/5969/414)

Abstract

An automatic sun tracking system was extended to a parabolic dish solar concentrator which can be used to cook or heat water. Parabolic dish solar concentrator has been in use couple of decades ago but has been tracking the sun manually. The automatic sun tracking system was incorporated on the parabolic dish with success and it works satisfactory. Every time the dish was left in the sun, it was found facing the sun as expected. These systems has been researched and developed before and applied on large scale applications like solar power generation plants and small electricity generation projects for remote areas which are not connected to national power grids.

Nomenclature

L_A	length of the actuator
r_1	moment arm length
x	position of actuator from the shaft
β	transmission angle
α	actuator inclination angle or coefficient of thermal expansion
θ	dish angular displacement angle
Φ	moment arm offset angle from the vertical dish axis (30°)
p	thread pitch
P	load or power
F	force
m	mass
M	bending moment
V	shear force
g	gravitational acceleration (9.81 m/s^2)
L	thread lead or length/distance
T	torque
t	time
σ	stress
ΔL	change in length
γ	dish inclination angle (22°)
ψ	thread included angle
N	actuator speed
μ	thread coefficient of friction
d	diameter
d_p	pitch circle diameter
ΔT	temperature difference
I	second moment of area
Z	section modulus
y	deflection
n	factor of safety
E	Young's modulus

Table of Contents

1. Introduction.....	12
2. Background study	12
2.1 Locating the sun in the sky	13
3. Objectives	14
4. Motivation for the current work.....	14
5. Literature review	15
5.1 Types of tracking	15
5.1.1 <i>Passive tracking</i>	15
5.1.2 <i>Active tracking</i>	16
a) Closed loop	16
i) V - Sensors	17
ii) Four quadrants method.....	17
b) Open loop	18
6. Tracking system design.....	19
6.1 Design decision.....	19
6.1.1 Tracking technique.....	19
6.1.2 Dish angular displacement during tracking	19
6.2 Tracking methodology.....	20
6.3 Design calculations and analysis	21
6.3.1 Actuator and tilting mechanism.....	22
a) Position analysis.....	12
b) Kinematics analysis	15
c) Screw torque analysis	19
6.3.2 Shaft and Frame	23
a) Reactions and pin sizing	25
b) Bending moment and deflections.....	28
c) Thermal effects	37
d) Bearing selection.....	36
e) Actuator mounting frame.....	36
7. Manufacturing methods	37
8. Assembly of components.....	38
8.1 Parabolic dish.....	38
8.2 Actuator.....	38

8.3 Solar panel	39
8.4 Painting	40
9. Safety	41
10. Testing and results	41
11. Cost analysis and payback time	43
11.1 Rural area customer	44
11.2 Urban area customer	44
12. Conclusions and recommendations.....	45
Appendix (drawings)	45
Bibliography	46

1. Introduction

The world is slowly but surely running out of fossil fuels e.g. oil, coal and/or natural gas, which are the sources of reliable energy that we use today. As the demand of energy keeps increasing so the price goes up too. In addition, the methods used to extract energy from these conventional energy sources pollute the environment, for example the burning of coal in thermal power plants produces carbon dioxide and carbon dioxide contributes to global warming. Apart from these fossil fuels are getting used up in the near future, are currently expensive and not environmental friendly. Therefore, alternative clean and sustainable energy source has to be found and/or developed. In the last decades, researchers have identified several renewable energy sources like solar energy, wind energy, hydro energy, biofuel, geothermal etc as potential clean energy sources. The disadvantages of these energy sources are that they are not reliable because they depend on the weather, weather patterns are erratic, hence difficult to predict, and they are inefficient.

In this project, the efficiency of solar energy as a source of energy for a water heating system will be increased by incorporating in an automatic sun tracking system. In the first phase of this project, a parabolic dish and a water heating system (pipe works, heat receiver and storage) were designed and constructed but the dish was tracking the sun manually. As a continuation on the project, the dish will be made to track the sun automatically.

For the dish to collect maximum heat energy, the sun rays must shine perpendicular to the dish aperture and since the sun is moving east to west daily and north to south annually, a sun tracking system is required to follow the sun and make sure that the dish always faces the sun.

2. Background study

For the dish to capture maximum solar radiation to heat water, it must face the sun in such a way that the sunrays are striking normal to the dish always. Since the sun appears (in fact it is the earth that is moving) to be moving from east to west daily and north to south annually, the dish must also move in the same direction and at the same speed as the sun so as to face the sun. The sun appears to move from east to west daily because the earth is rotating on its axis making a complete rotation in 24 hours. It also appears to move from north to south annually because the

earth is revolving around the sun and its axis of rotation is tilted 23.5° from the vertical (see figure 1).

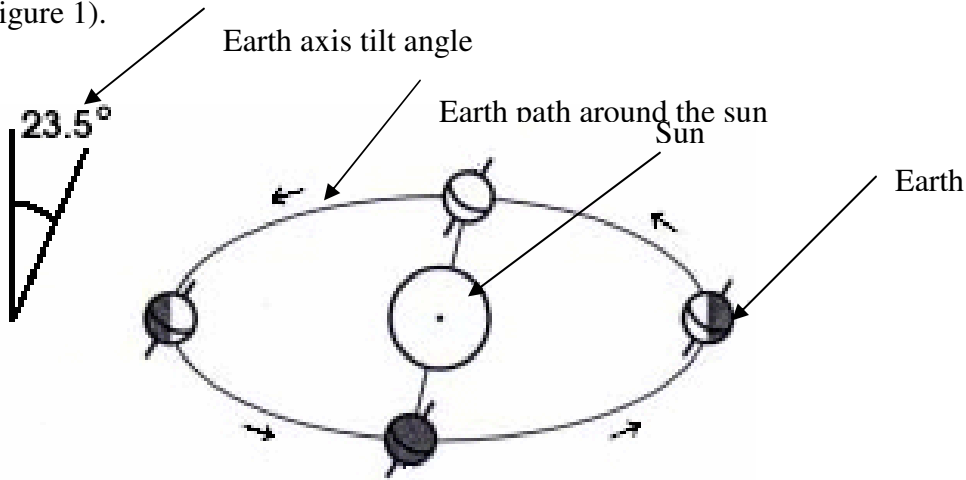


Figure 1. Earth movement [1]

2.1 Locating the sun in the sky

The position of the sun in the sky is located by two angles [2]: azimuth angle and the sun elevation angle. In order to visualize these angles, consider the earth to be a circular disc (horizon) and let it be enclosed by a hemisphere with the sun attached on the inner surface of the hemisphere as shown in Figure 2. It can also be seen that the sun travels in a different path every day of the year. The extreme paths are the tropic of Capricorn and the tropic of Cancer, so during the year, the sun take paths between the two extremes.

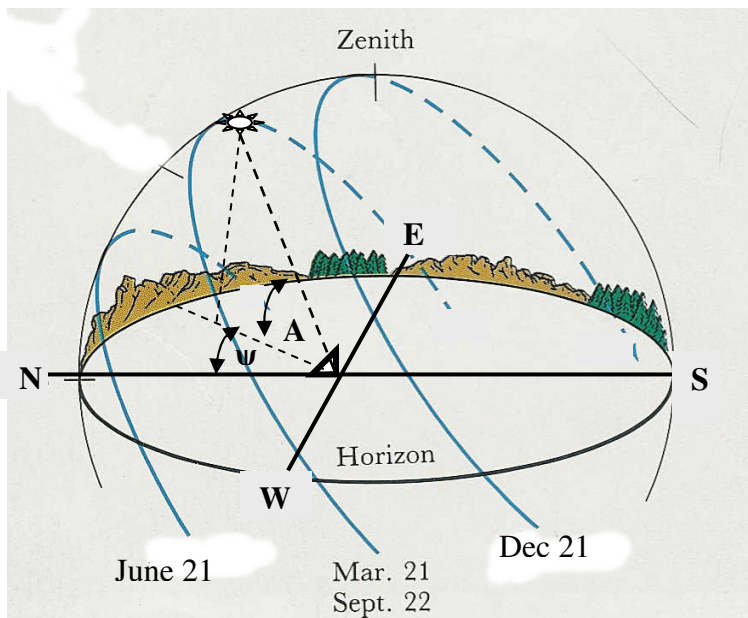


Figure 2. Sun position in the sky [3]

If we consider the dish to be at the center of the disc (earth), it follows that two angles are required to define the sun position from the dish any time during the day and year in the solar coordinate system. These angles are the azimuth angle (ψ), which is the projection of the sun on the horizon measured clockwise from line SN as a reference and the sun elevation angle “A” measured from the horizon plane to the sun ray(s).

Therefore, for tracking to be realised, the tracking system must be able to orient the parabolic dish at the right angles that coincides with those of the sun at the right time.

3. Objectives

The objective of this project is to design, construct and test an automatic sun tracking system. The tracking system should be able to track the sun as it travels across the sky east to west daily and north to south annually with reasonable accuracy. The parabolic dish designed and manufactured in the first phase of this project will be mounted on the designed system so that it can track the sun on its own.

4. Motivation for the current work

- In the first phase of this project, the dish was tilted manually to track the sun, so every time a person has to be positioned next to the dish to tilt it to face the sun which is unpleasant, boring and can be even dangerous if a person happens to look at the focal point with his/her naked eyes. The positions of the sun were not determined to guide tilting of the dish, so one cannot determine whether the dish is correctly facing the sun or not. When the dish does not face the sun correctly, the amount of heat that can be collected is reduced. With automatic tracking, all these shortcomings will be avoided.
- Manually sun tracking solar cookers using parabolic dishes are used in Namibia (figure 3) [4], so should this project be a success, the tracking system can be integrated onto these solar cookers.



Figure 3. Parabolic solar cooker [4]

- Another reason why this project should/must go ahead is that, it will be useful as demonstration tool at the science and career fairs that are held annually at the Polytechnic of Namibia and also as a teaching aid e.g. to conduct experiments on solar energy and heat transfer related studies.
- Finally, sun tracking increases the energy collected by the collector by 30-40%, compared to the collector without a tracking system [5]

5. Literature review

The preliminary research in the literature indicates that sun-tracking systems are already in use in Namibia and beyond. It was also revealed that there are different types of sun tracking systems with different controls and equipments. In the next paragraphs, these tracking systems will be briefly discussed.

5.1 Types of tracking

5.1.1 Passive tracking

Passive tracking is a system of collecting sunlight using static, non-moving, and non-tracking systems for example solar panels on a building. These devices rely on their position to most effectively capture sunlight e.g. some panels are positioned to capture sunlight before noon while others are positioned to capture the sunlight afternoon. All panels are fixed in their positions. Architectural considerations are critical in the effectiveness of passive tracking [6].

There is also a type of tracking that involves movement, but it is classified as passive tracking because there is no input drive from the motor involved. “The device consists of a two-axis gimbal system (see figure 4) with its orientation controlled by interconnected ballasts filled with a volatile fluid” e.g. chlorofluorocarbon (CFC), liquid petroleum gas (LPG) or butane. “Accurate focusing is realized by ensuring that each significant mass element is balanced by another element of equal mass equidistant from and diametrically opposite to it through the point of intersection of the two-gimbal axes for all possible orientations of the system” [7].

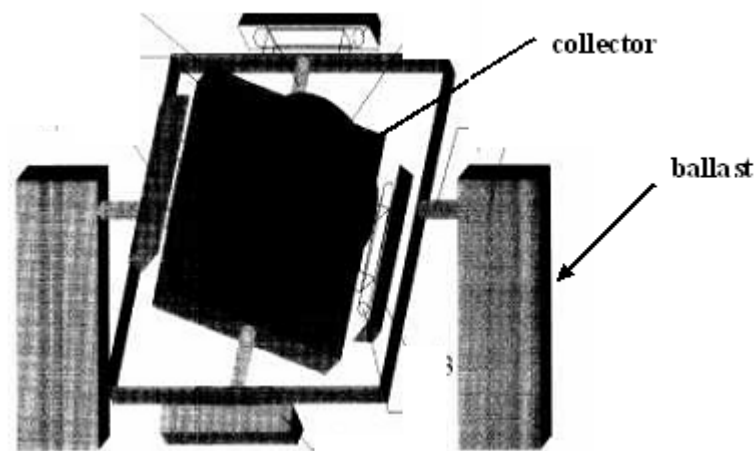


Figure 4 an example of passive tracking [7]

However, the use this tracking system has declined in recent years since people realized that CFC damages the ozone layer and it does not work well in cold weather, and other gases are flammable. In addition, it takes time to react to the change in the sun position [8]

5.1.2 Active tracking

This tracking method is further divided into two groups: closed loop and open loop system depending on how the tracking mechanism motion is controlled.

a) Closed loop

In this tracking method, photoresistor sensors determine the sun position, these sensors send a signal(s) to a controller that controls the stepper motor (s) that rotates the collector to face the sun. Normally two sensors are required for single axis (east – west only) tracking and four sensors for double (east – west and north – south) axis tracking [9]. These sensors are photoresistor or Light Dependent Resistors (LDR), which are resistors whose resistance depends

on the light intensity available. When the light intensity is more, the resistance increases and as result, less current is passing through and in poor light intensity, it is the opposite.

Sensors can be arranged in different ways to suite the designer, now lets look at some of the commonly used arrangements:

i) V - Sensors

Sensors are arranged in pairs in a vee configuration on the collector in such a way that when the sun is shining perpendicular to the collector, all sensors in a pair are receiving same light intensity hence the current in both sensors is same [10].

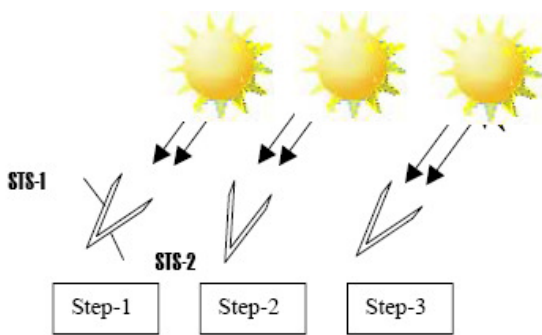


Figure 5 V – sensors [10]

Step – 1 the sun is shining perpendicular to the collector, all sensors in a pair are receiving same light intensity hence the current in both sensors is same.

Step – 2 now the sun moves and STS -1 is receiving more light than STS – 2 and the current through the sensors is not equal, also the collector is no longer facing the sun.

Step – 3 the stepper motor rotate the collector to face the sun and the current through the sensors is equal again. When the sun moves again, the same procedures are repeated.

ii) Four quadrants method

As the name depicts, sensors are arranged in four quadrants as shown in figure 6 below.

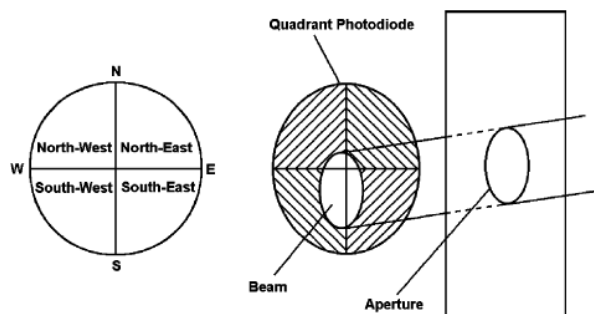


Figure 6 four quadrants sensors [11]

With this method, the sensors are covered with an object with a hole in it and it is directly above the centre where sensors meet. The sun shines on the sensors through this hole and when the collector is facing the sun, the illuminated area on all sensors is equal. When the sun moves, the sun rays are no longer normal to the hole aperture and as a result, the illuminated areas of the sensors are not equal anymore. The stepper motor will then rotate the collector until all illuminated areas are equal.

When the sun moves again, the same procedures are repeated.

This method is called a closed loop system, because there is feedback, before the stepper motor stop rotating, the controller makes sure that the collector is facing the sun when the current in the resistors is same.

The closed loop tracking is easy to install because not much alignment is required as the sensors seek the sun themselves. However the wear and tear is more because there is lot of moving time.

b) Open loop

Unlike the closed loop tracking system, the open loop tracking does not use sensors to locate the sun, it make use of a formula (fixed algorithms) to determine the position of the sun from the predetermined inputs and the corresponding outputs. These inputs are date of the year, time of the day and location of the place e.g. latitude and longitude, while the outputs are the azimuth and the elevation angles of the sun. The formula determines the path of the sun and it is programmed in the controller that incorporates a timer. Like the closed loop system, the controller controls the stepper motor(s) that rotate the collector [9].

Since the outputs are predefined, there is no feedback in this system hence the name open loop.

By looking at the types of tracking discussed above, it can be seen that it is only the open loop tracking that requires the azimuth and elevation angles to be determined. In the closed loop tracking, the sensors themselves locate these angles by seeking the sun, although they don't display them, so they don't have to be determined.

The open loop tracking technique is more accurate than the other technique presented before provided that the algorithm is correct and accurate. However it is more complicated to program and install. Also if something goes wrong with the program, an expert is needed to fix it.

6. Tracking system design

The research has revealed many sun tracking technique to choose from, therefore a decision has to be made based on available resources and requirements.

6.1 Design decision

6.1.1 Tracking technique

By considering the advantages and disadvantages of tracking systems discussed above and the intended use of the system, the closed loop tracking technique was chosen to track the east-west movement of the sun and the passive tracking for the north – south movement of the sun.

A closed loop is chosen because there is no programming required as the actions of the sensors are already predefined by the manufacturer as explained in section 5.1.2 a) i) early, they are easy to install and maintain and the set up is simple for the end user to use. V-sensor arrangement is used because they are available in the local market.

For the passive tracking, the parabolic dish is inclined facing north at an angle equal to the latitude of the place. Since Windhoek is located at 22°S, the dish will be inclined at 22° from the horizontal facing north because Namibia is on the southern hemisphere. This passive tracking is appropriate because the focal point of the dish is inside the dish and the receiver will be stationary. If the dish were rotating north – south also, then the receiver must rotate as well.

In this design, the sacrifice was made on the wear and tear associated with the closed loop and the replacement of the sensors at some time to for the advantages mentioned above.

6.1.2 Dish angular displacement during tracking

In order to decide through which angle should the dish rotates, the availability of solar radiation in Windhoek was considered. Table 1 shows the availability of solar radiation in Windhoek for two days, one in winter and the other in summer from 08:30 in the morning to 15:30 in the afternoon.

Table 1. Solar energy in Windhoek [12]

Time of the day	Voltage (V)	Solar intensity (W/m ²) 14/07/2009	Solar intensity (W/m ²) 08/10/2009
08:30 am	0.038	351.85	448
09:30 am	0.062	574.07	693
10:30 am	0.076	703.70	854
11:30 am	0.084	777.78	977
12:30 pm	0.083	768.52	1032

13:30 pm	0.072	666.67	1056
14:30 pm	0.059	546.30	836
15:30 pm	0.037	342.59	236

From the table, it can be seen that the solar intensity increase with time during the morning until some maximum value is reached and then decrease in the afternoon. The solar intensity is maximum at around noon. Also using the sun position diagram, it was found that during peak solar intensity duration, the sun covers approximately 100° of angular displacement. Hence the tracking system covers this angle.

6.2 Tracking methodology

The schematic diagram of the system (without a receiver) is shown in Figure 7 below.

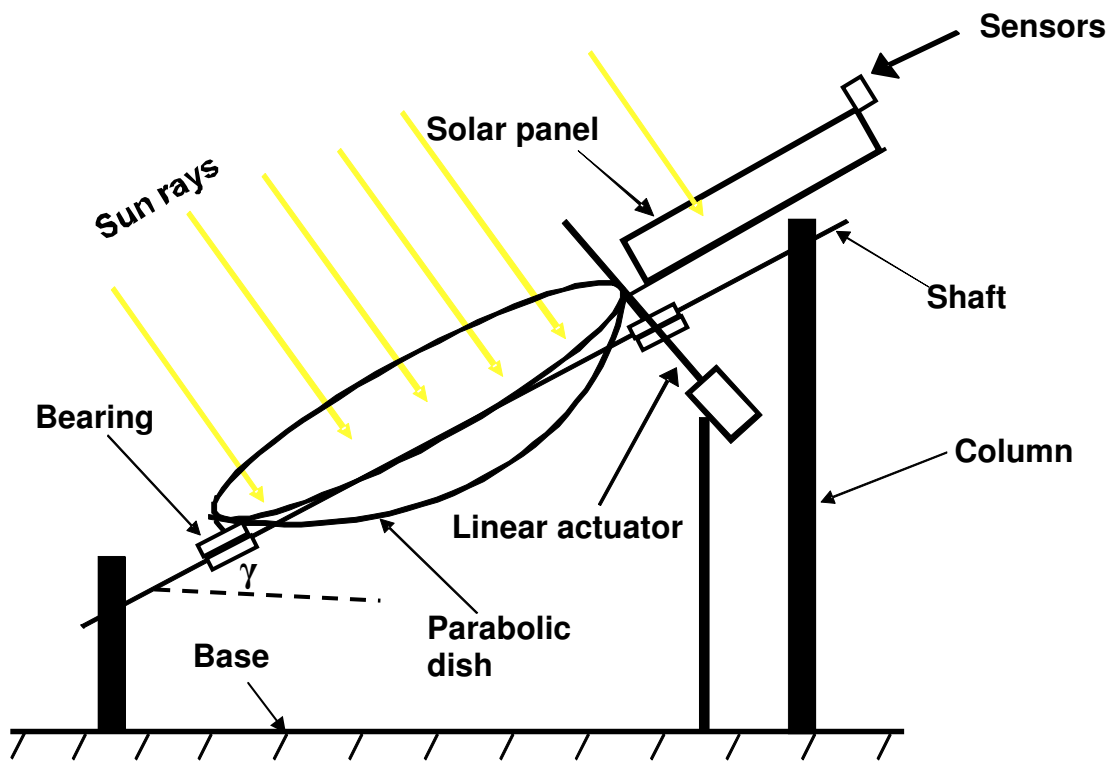


Figure 7. Schematic diagram of the system

Sensors seek the sun and send signals to the linear actuator through the controller. A linear actuator driven by a DC motor rotates the dish. The controller changes polarities across the motor terminals depending on the sun's position in the sky, and allows the dish to rotate east – west (actuator extend) and west – east (actuator shorten).

Since the system must be free from conventional energy sources, the actuator motor is powered by a solar charged battery.

The parabolic dish is mounted on the shaft by flanged-ball bearings. The solar panel and the sensor are bolted on the dish and together they rotate as an integral unity. This integral unity is then connected to the actuator through a moment arm.

The solar panel and parabolic dish rotate together because the solar panel must track the sun as well to charge the actuator motor battery.

Apart from the automatic tracking, the system shall have a manual mode also in case the tracking system is faulty:

- If the tracking system is faulty, the actuator shall be decoupled from the moment arm to rotate the dish with hands. Manual locking knob will be provided for this.

Since the actuator is not designed to cover for the entire sun interval, a limit switch is placed to switch off the actuator when the solar intensity has reduced and the sun is about to go down the horizon.

6.3 Design calculations and analysis

The actuator was designed and positioned to give required motion characteristics while strength analyses on the shaft were also performed. In this project the emphasis is mainly on performance, therefore no strength analysis were done on mounting frames. Frames were assumed strong enough because no load shall be applied heavier than food and/or water.

The following information's and/or design parameters were known prior to the design:

Table 2. Known design parameters

Quantity	Magnitude
Dish inclination angle	22°
Dish angular displacement during tracking	90°
Dish mass	2 kg
Dish centre of mass from the shaft axis	44 mm
Focal point	200 mm
Dish diameter	1000 mm
Dish height	310 mm
Motor voltage rating	12 V
Motor current rating	1.7 A
Motor speed	100 rpm
Motor weight	3N
Steel density	7850kg/m ³
Gravitational acceleration	9.81 m/s ²

The centre of gravity of the dish from the axis	44 mm
Solar panel mass	2 kg

The actuator motor was taken from the automobile door window sourced from the local car spares center and it was modified to fit this application. The motor was tested in the electrical engineering laboratory to determine its speed, and current as indicated above. The voltage was already indicated on the specification.

6.3.1 Actuator and tilting mechanism

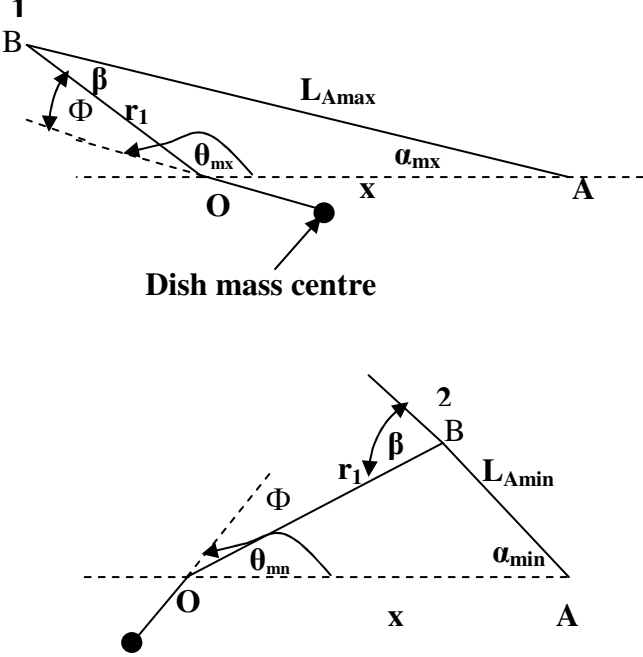
The design of the actuator and the tilting mechanism is a four bar linkage which is a motion generation problem because a line orientation, which is a dish vertical axis is being controlled. Because this line is rotating about a fixed point (shaft axis), The tilting mechanism was designed to rotate the dish to its required extreme points without reaching a toggle position.

Although results presented in this report are from straight forward calculations, iterations were done considering the motor torque and space constraint.

The following design limits were considered in designing the mechanism to rotate the dish through 90°:

- The distance between the shaft and the actuator must be less than 400 mm because the frame where the dish will be mounted is already available with this dimension.
- The motor must only rotate in one direction when the dish is rotating from side to side.
- The torque required to rotate the dish must not exceed the motor torque
- The angular rotation of the dish must be low and smooth so that the dish does not stop in a jerky manner when the motor stops during operations.
- Both positions, kinematics and kinetics constraints have to be satisfied by the design

a) Position analysis

Initial data	Calculations and sketches	Results
<p> $x = 370 \text{ mm}$ $r_1 = 180 \text{ mm}$ $\theta_{\max} = 130^\circ$ $\theta_{\min} = 40^\circ$ $\Phi = 30^\circ$ $\angle(AOB) = \theta - \Phi$ </p>	<p>Consider the actuator positions at the dish extreme positions, such that the angle between these extreme positions is 90°:</p>  <p style="text-align: center;">Figure 8. Actuator positions analysis</p> <p>The moment arm OB is mounted on the shaft at O and pinned to the actuator at B, while the actuator AB is fixed at A. The moment arm is shifted from the dish axis by angle Φ to increase the transmission angle β. The maximum and minimum L_A, α and β at the extreme positions of the mechanism must be determined:</p>	<p> $L_{A\max} = 438 \text{ mm}$ $L_{A\min} = 195 \text{ mm}$ $\alpha_{\max} = 23.9^\circ$ $\alpha_{\min} = 9.2^\circ$ $\beta_1 = 56.1^\circ$ $\beta_2 = 19.2^\circ$ </p>

L_A - length of the actuator

r_1 – moment arm length

n – position of actuator from the shaft

β – transmission angle

α – actuator inclination angle

From the cosine rule, the actuator length become:

$$L_A^2 = n^2 + r_1^2 - 2nr_1\cos(\theta - \phi) \quad (1)$$

Substituting θ_{\max} and θ_{\min} in (1), the maximum and minimum length:

$$\begin{aligned} L_{A\max} &= \sqrt{0.37^2 + 0.18^2 - 2 \times 0.37 \times 0.18 \cos(130 - 30)} \\ &= 0.438 \text{ m} \end{aligned}$$

$$\begin{aligned} L_{A\min} &= \sqrt{0.37^2 + 0.18^2 - 2 \times 0.18 \times 0.37 \cos(40 - 30)} \\ &= 0.195 \text{ m} \end{aligned}$$

Using the sine rule, the actuator inclination angle α :

$$\frac{\sin\alpha}{r_1} = \frac{\sin(\theta - \phi)}{L_A} \quad (2)$$

Substituting the extreme values of θ and L_A in (2) and make α the subject of the formula:

$$\alpha_{\text{mxn}} = \sin^{-1}\left(\frac{\sin(130 - 30) \times 180}{273}\right)$$

$$= 23.9^\circ$$

$$\alpha_{\text{mxn}} = \sin^{-1}\left(\frac{\sin(40 - 30) \times 180}{195}\right)$$

$$= 9.2^\circ$$

Finally, the transmission angle must complete the triangle:

$$\beta_1 = 180 - \alpha - \angle AOB$$

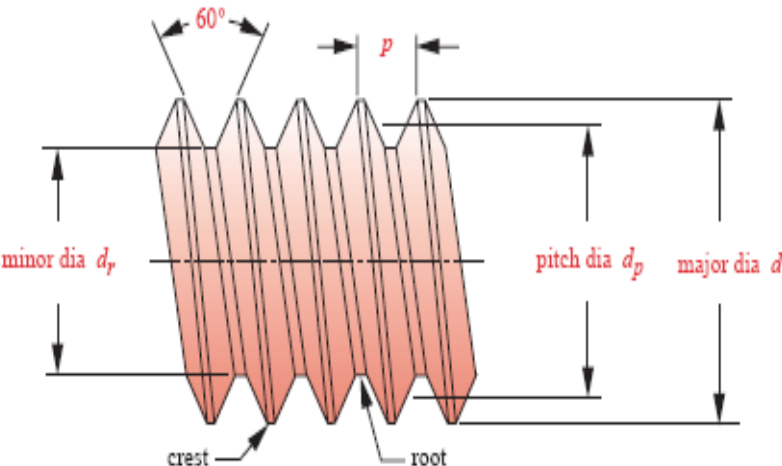
$$= 180 - 23.9 - 100 = 56.1^\circ$$

$$\beta_2 = 180 - \alpha - \angle AOB$$

$$= 180 - (180 - 9.2 - 10) = 19.2^\circ$$

Therefore the actuator will be 438 mm long and it will be fixed 370 mm from the shaft. The moment arm is 180 mm.

b) Kinematics analysis

Initial data	Calculations and sketches	Results
<p>N = 100 rpm</p> <p>$L_{Amax} = 438$ mm</p> <p>n = 370 mm</p> <p>$r_1 = 180$ mm</p> <p>The thread pitch was chosen from the thread table as: Pitch = 1.5 mm</p>	<p>The actuator is made up of a lead screw and a nut with metric threads. When the screw is turned by the motor, the nut will move axially relative to the screw and the moment arm shall be pinned to the nut. In figure 9 below is the typical thread of the actuator lead screw.</p>  <p style="text-align: center;">Figure 9. Screw threads</p> <p>In figure 9. P is the pitch of the thread and its chosen as 1.5 mm and the thread has an included angle of 60°.</p> <p>For the thread shown above, the lead “L” is equal to the pitch because it’s a single start thread. A lead is a distance the nut will advance axial in one rotation of the screw.</p>	

Therefore the velocity of the nut on the screw is:

$$V_{\text{nut}} = \frac{NL}{60 \text{ seconds}} = \frac{100 \times 1.5}{60} = 2.5 \text{ mm/s} \quad (3)$$

This velocity is equal to the rate at which the actuator length is changing with time and it is constant as long as the pitch and the motor rpm do not change. So

$$V_{\text{nut}} = \dot{L}_A = 2.5 \text{ mm/s}$$

To get the time taken between the two extreme positions:

$$t = \frac{L_{A\text{max}} - L_{A\text{min}}}{\dot{L}_A} = \frac{438 - 195}{2.5} = 97.2 \text{ s} \quad (4)$$

Figure 8 is repeated again in figure 9 showing the velocities of the components. Now the angular velocity of the moment arm (ω_{OB}) and that of the actuator (ω_{AB}) will be determined.

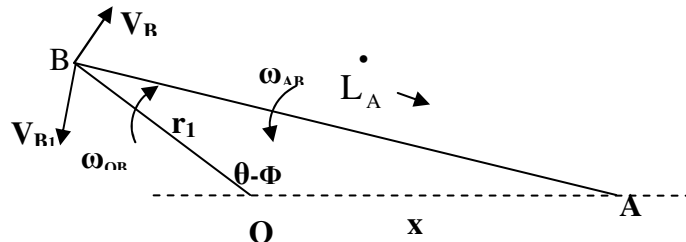


Figure 10. Actuator kinematics

To get the angular velocity of OB, equation (1) is differentiated with respect to time:

$$L_A^2 = x^2 + r_1^2 - 2xr_1 \cos(\theta - \phi)$$

$$2\dot{L}_A L_A = 2xr_1 \dot{\theta} \sin(\theta - \phi)$$

$$\dot{L}_A = 0.0025 \text{ m/s}$$

$$t = 97.2 \text{ s}$$

$$(\omega_{OB})_1 = 0.017$$

rad/s

$$(\omega_{OB})_2 = 0.042$$

rad/s

Since Φ is a constant ω_{OB} is equal to $\dot{\theta}$:

$$\dot{\theta} = \omega_{OB} = \frac{L_A \dot{L}_A}{r_1 \sin(\theta - \phi)} \quad (5)$$

For the two extreme positions, ω_{AB} is found by substituting L_A and θ at those positions:

$$(\omega_{OB})_1 = \frac{438 \times 2.5}{370 \times 180 \sin(130 - 30)}$$

$$= 0.017 \text{ rad/s}$$

$$(\omega_{OB})_2 = \frac{195 \times 2.5}{370 \times 180 \sin(40 - 30)}$$

$$= 0.042 \text{ rad/s}$$

For the angular velocity of the actuator, first the velocity of point B must be determined:

From point O, V_B becomes:

$$V_B = \omega_{OB} \times r_1 \quad (6)$$

Substituting the values of ω_{OB} from (5):

$$V_{B1} = 0.017 \times 0.18 = 0.00306 \text{ m/s}$$

$$V_{B2} = 0.042 \times 0.18 = 0.00756 \text{ m/s}$$

From point A, velocity of point B is observed to equal to:

$$\vec{V}_{B^1} = \vec{V}_B + \dot{L}_A = \omega_{AB} \times L_A \quad (7)$$

Since \vec{V}_B and \dot{L}_A are orthogonal, it follows that:

$$\vec{V}_B^2 + \dot{L}_A^2 = (\omega_{AB} \times L_A)^2$$

$$\omega_{AB} = \sqrt{\frac{\vec{V}_B^2 + \dot{L}_A^2}{L_A^2}}$$

Hence:

$$(\omega_{AB})_1 = \sqrt{\frac{0.00306^2 + 0.0025^2}{0.438^2}}$$

$$= 0.006 \text{ rad/s}$$

$$(\omega_{AB})_2 = \sqrt{\frac{0.00756^2 + 0.0025^2}{0.195^2}}$$

$$= 0.018 \text{ rad/s}$$

$$(\omega_{AB})_1 = 0.006 \text{ rad/s}$$

$$(\omega_{AB})_2 = 0.018 \text{ rad/s}$$

The linear velocity of the actuator is 2.5 mm/s and it will take 97.2 seconds to rotate the dish between its extreme positions when the motor is run continuously.

c) Screw torque analysis

In this analysis, the torque required to rotate the system will be determined by assuming the pitch diameter of the screw and compare to the torque rating of the motor.

Initial data	Calculations and sketches	Results
<p> $r_1 = 180 \text{ mm}$ $r_2 = 34 \text{ mm}$ $r_3 = 44 \text{ mm}$ $\beta_1 = 56.1^\circ$ $\beta_2 = 19.2^\circ$ mass of dish = 2 kg $g = 9.81 \text{ kg/m/s}^2$ motor voltage = 12 V motor current = 1.7 A $N = 100 \text{ rpm}$ $L = 1.5 \text{ mm}$ $\mu = 0.15$ Thread angle $\psi = 60^\circ$ $d_p = 12 \text{ mm}$ </p>	<p> Motor power (P) = voltage(V) \times current(I) $P = VI$ (8) $= 12 \times 1.7 = 20.4 \text{ W}$ The panel and its mounting brackets were estimated as a homogeneous box with a mass of 5 kg. The torque from the motor is determined from: $T = \frac{P}{\omega} = \frac{20.4 \times 60}{2\pi n} = 1.95 \text{ Nm}$ (9) In order to get the torque required to rotate system between its extreme positions, consider the free body diagram of the shaft and its loading, which is the 2 kg dish and 5 kg panel. Since the dish is mounted in bearings, the rotation can be assumed friction less. </p>	<p> Power = 20.4 W $T_{\max} = 1.95 \text{ Nm}$ </p>

Lowering

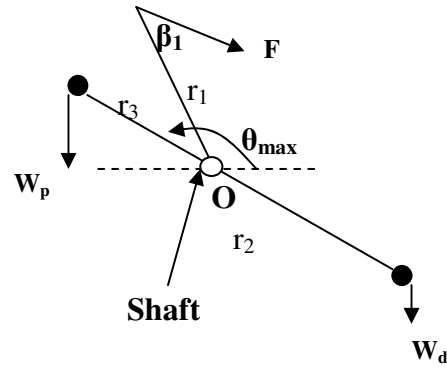


Figure 11. Lowering the dish

$$T_d = 0.079 \text{ Nm}$$

Where F is the force required to rotate the system.

$$\sum M_o = 0 \tag{10}$$

$$W_d r_d \cos(180 + \theta) + W_p r_p \cos\theta + F r_1 \sin\beta_1 = 0$$

$$F = \frac{W_d r_d \cos(180 + \theta) + W_p r_p \cos\theta}{-r_1 \sin\beta_1}$$

$$= \frac{2 \times 9.81 \times 0.044 \cos(180 + 130) + 5 \times 9.81 \times 0.034 \cos 130}{-0.18 \sin 56.1}$$

$$= 3.5 \text{ N}$$

For a lead screw, the torque to lower a load is given by:

$$T_d = \frac{F d_p}{2} \left[\frac{(\mu \pi d_p - L \cos \psi)}{(\mu d_p \cos \psi + \mu L)} \right] \tag{11}$$

$$= \frac{3.5 \times 0.0109}{2} \left[\frac{0.15 \times \pi \times 0.012 - 0.0015 \cos 60}{0.15 \times 0.012 \times \cos 60 + 0.15 \times 0.0025} \right]$$

$$= 0.079 \text{ Nm}$$

This 96% less than the motor output torque

Lifting

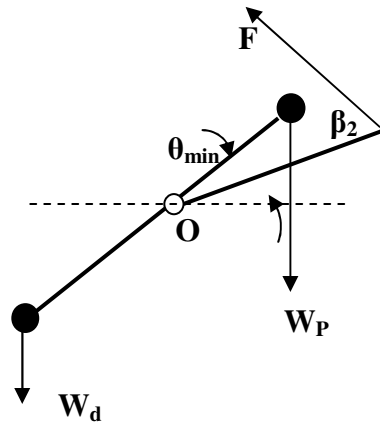


Figure 12. Lifting the dish

$$\sum M_o = 0$$

$$W_d r_d \cos(180 + \theta) + W_p r_p \cos \theta - F r_l \sin \beta_2 = 0$$

$$F = \frac{W_d r_d \cos(180 + \theta) + W_p r_p \cos \theta}{r_l \sin \beta_2}$$

$$= \frac{2 \times 9.81 \times 0.044 \cos(180 + 40) + 5 \times 9.81 \times 0.034 \cos 40}{0.18 \sin 19.2}$$

$$= 10.4 \text{ N}$$

For a lead screw, the torque to lower a load is given by [13]:

$$T_u = \frac{F d_p}{2} \left[\frac{(\mu \pi d_p + L \cos \psi)}{(\mu d_p \cos \psi - \mu L)} \right] \tag{12}$$

Where μ is the thread coefficient of friction

$$= \frac{12.1 \times 0.0109}{2} \left[\frac{0.15 \times \pi \times 0.012 - 0.0015 \cos 60}{0.15 \times 0.012 \times \cos 60 + 0.15 \times 0.0025} \right]$$

$$= 0.56 \text{ Nm}$$

$$T_u = 0.56 \text{ Nm}$$

The screw is self-locking

This 71 % less than motor output torque. Since both the torque required to lower and lift the dish are less than 70 % the motor torque (9), the chosen geometry is good enough.

For the screw to be self – locking, the following condition must be satisfied:

$$\mu \geq \frac{L \cos \psi}{\pi d_p} \quad (13)$$

$$\frac{1.5 \cos 60}{\pi \times 10.9} = 0.022$$

Since 0.022 is less than 0.15, the actuator is self locking, it will not back drive due to an axial applied load.

The thread inclination angle is given by:

$$\lambda = \tan^{-1} \left(\frac{L}{\pi d_p} \right) = \tan^{-1} \left(\frac{1.5}{10.9\pi} \right) = 2.5^\circ \quad (14)$$

6.3.2 Shaft and Frame

A dish and the absorber are to be mounted on the shaft, which is a non-prismatic composite of members in series (see figure 13) simply supported on both ends on 32×32×2 mm rectangular columns.

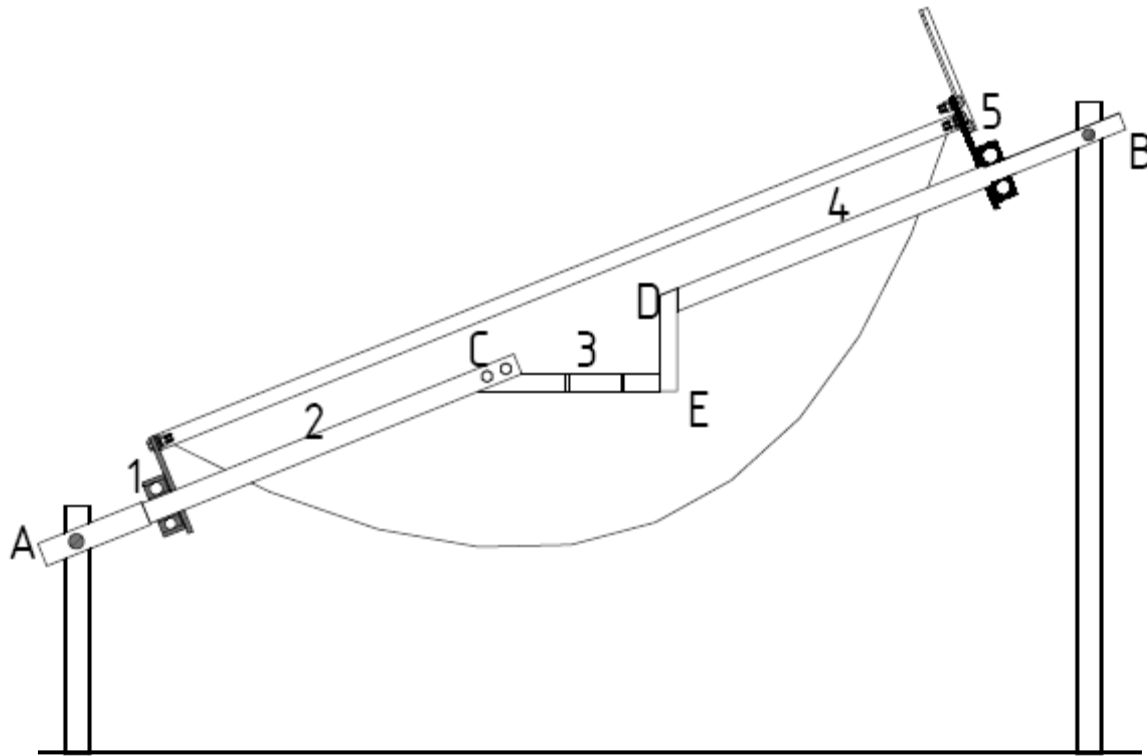


Figure 13. A section through the dish assembly

The shaft is designed with that shape because it is inclined and it is supporting a rotating member (parabolic dish) and the absorber that must frame perpendicular to the horizontal. It is made up of two stepped rods AC (28 mm to 25 mm) and DB (25 mm to 20 mm) and rectangular plates CE and DE which are 6 × 20 mm.

A dish shall be supported on flanged deep groove-ball bearings at the steps (1 and 5) so that the rotation is friction less, while the absorber shall sit on member CE at point 3 so that it frames straight up on the inclined axel.

Member BD, DE and EC are to be welded together at points D and E respectively, while member AC shall be bolted to member CB at C. This is because during the assembly, the bearing at 1 will pass at C. For details on how the parts are assembled together, see the drawings.

Calculations were carried out to size the pins at A and B, the bolts at C as well as to determine the bending moment and the deflection of the non-prismatic composite shaft. The shaft is subjected to concentrated loads at points 1, 2, 3, 4 and 5. Let's denote these loads as P_1, \dots, P_5

P_1 is the load at the bottom bearing and it is equal to half the dish weight (2 kg), the bearing weight (0.6 kg), moment arm (0.2 kg) and bottom mounting plate weights (1 kg):

$$P_1 = 9.81(2(0.5) + 0.6 + 0.2 + 1) = 27.5 \text{ N}$$

P_2 is the load due to the weight of AC treated as a concentrated load at the centre of gravity of the rod:

$$P_2 = g\rho V = 9.81 \times 7800 \times \pi \times 0.028^2 \times 0.25 \times 0.593 = 27.9 \text{ N}$$

P_3 is the load due to the weight of water in the absorber neglecting the absorber weight and that of the plates CE and ED:

$$P_3 = g\rho V = 9.81 \times 1000 \times \pi \times 0.05^2 \times 0.3 = 23.1 \text{ N}$$

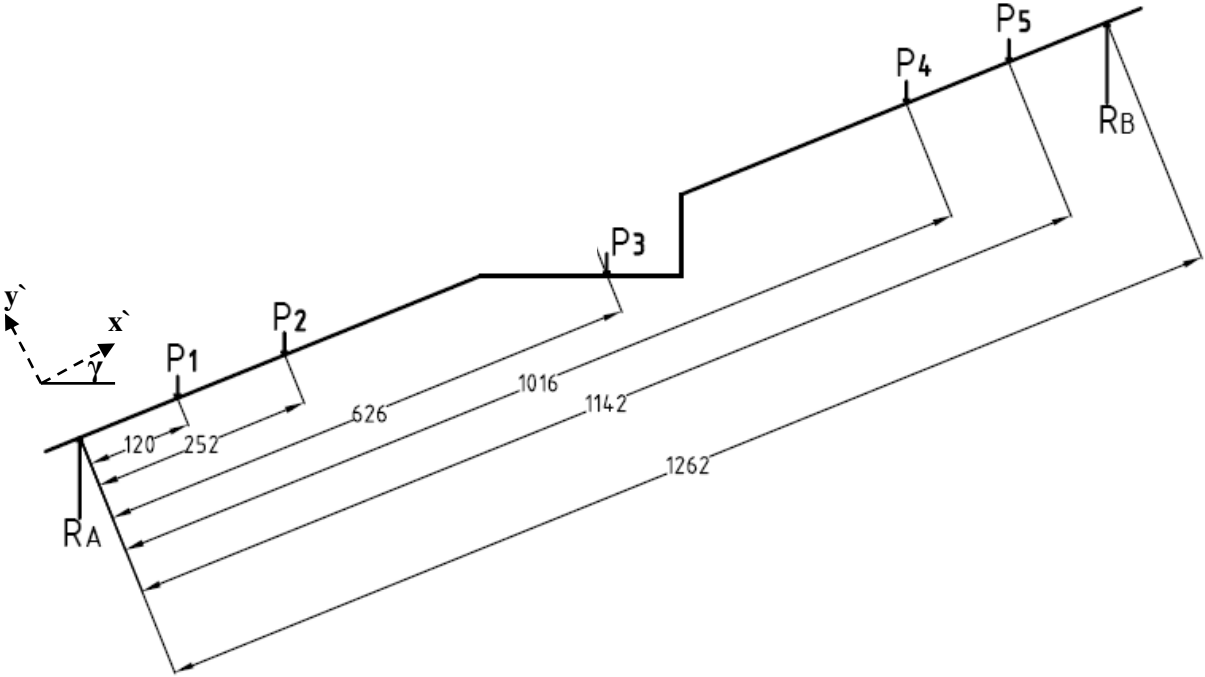
P_4 is the load due to the weight of DB treated as a concentrated load at the centre of gravity of the rod:

$$P_4 = g\rho V = 9.81 \times 7800 \times \pi \times 0.028^2 \times 0.25 \times 0.582 = 27.4 \text{ N}$$

P_5 is the load at the top bearing and it is equal to half the dish weight (2 kg), the bearing (0.48 kg), solar panel and its brackets (5 kg):

$$P_5 = 9.81(2(0.5) + 0.48 + 5) = 63.6 \text{ N}$$

a) Reactions and pin sizing

Initial data	Calculations and sketches	Results
<p><i>Loads</i></p> <p>$P_1 = 27.5 \text{ N}$ $P_2 = 27.9 \text{ N}$ $P_3 = 23.1 \text{ N}$ $P_4 = 24.4 \text{ N}$ $P_5 = 63.6 \text{ N}$</p> <p>$\gamma = 22^\circ$</p> <p>$a_1 = 120 \text{ mm}$ $a_2 = 251.5 \text{ mm}$ $a_3 = 626 \text{ mm}$ $a_4 = 1016 \text{ mm}$ $a_5 = 1142 \text{ mm}$ $L = 1262 \text{ mm}$</p> <p><i>Factor of safety:</i></p> <p>$n = 4$</p> <p><i>Steel yield</i></p>	<p>Now let's consider the free body diagram of the shaft with the loads and their distances from "A" indicated.</p>  <p style="text-align: center;">Figure 14. Shaft free body diagram</p> <p>The reaction forces R_A and R_B are then determined from the equilibrium of the shaft:</p> $\sum M_A = 0 \tag{15}$	<p>$R_A = 70.3 \text{ N}$ $R_B = 99.2 \text{ N}$</p>

$$\frac{\sigma_y}{n} = \frac{R_B}{2A} \quad (17)$$

Where n is the factor of safety and A is the cross-sectional area of the pin.

Expressing the area in terms of the diameter: $A = \frac{\pi d^2}{4}$, substituting in (17) and make d the subject

of the formula:

$$\begin{aligned} d &= \sqrt{\frac{2nR_B}{\pi\sigma_y}} \\ &= \sqrt{\frac{2 \times 4 \times 99.2}{\pi \times 340 \times 10^6}} \\ &= 0.862 \times 10^{-4} \text{ m} \\ &= 0.862 \text{ mm} \end{aligned}$$

These forces are very small and their effect is negligible and they don't dictate the design, an 8 mm pin was selected

b) Bending moment and deflections

Initial data	Calculations and sketches	Results
<p><i>Loads</i></p> <p>$P_1 = 27.5 \text{ N}$</p> <p>$P_2 = 27.9 \text{ N}$</p> <p>$P_3 = 23.1 \text{ N}$</p> <p>$P_4 = 24.4 \text{ N}$</p> <p>$P_5 = 63.6 \text{ N}$</p> <p>$R_A = 70.3 \text{ N}$</p> <p>$R_B = 99.2 \text{ N}$</p> <p>$\gamma = 22^\circ$</p> <p><i>Factor of safety:</i></p> <p>$n = 4$</p> <p><i>Steel yield stress:</i></p> <p>$\sigma_y = 340 \text{ MPa}$</p>	<p>In order to determine the bending moment and the deflection of the shaft, the loads and the reactions were resolved into components in the plane $x' y'$ where the shaft will bend.</p> <p>Since the shaft will only bend in the y' direction, the components of the loads in these directions become:</p> <p>$P_1' = 27.5 \cos 22 = 25.5 \text{ N}$</p> <p>$P_2' = 27.9 \cos 22 = 25.9 \text{ N}$</p> <p>$P_3' = 23.1 \cos 22 = 21.4 \text{ N}$</p> <p>$P_4' = 27.4 \cos 22 = 25.4 \text{ N}$</p> <p>$P_5' = 63.6 \cos 22 = 59 \text{ N}$</p> <p>$R_A' = 70.3 \cos 22 = 65.2 \text{ N}$</p> <p>$R_B' = 99.2 \cos 22 = 92 \text{ N}$</p>	

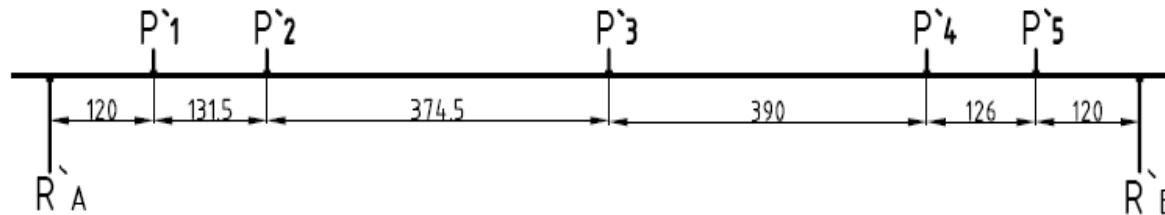


Figure 15. Load diagram

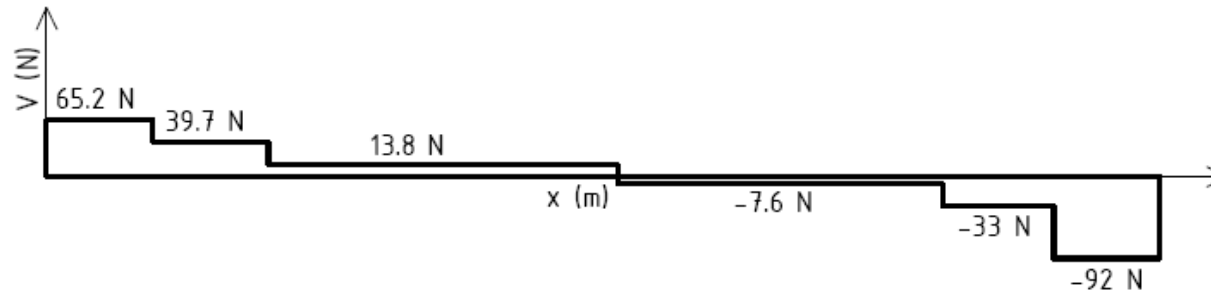


Figure 16. Shear force diagram

$$V_A = R_A = 65.2 \text{ N}$$

$$V_1 = V_A - P_1 = 65.2 - 25.5 = 39.7 \text{ N}$$

$$V_2 = V_1 - P_2 = 39.7 - 25.9 = 13.8 \text{ N}$$

$$V_3 = V_2 - P_3 = 13.8 - 21.4 = -7.6 \text{ N}$$

$$V_4 = V_3 - P_4 = -7.6 - 25.4 = -33 \text{ N}$$

$$V_5 = V_4 - P_5 = -33 - 59 = -92 \text{ N} = R_B = V_B$$

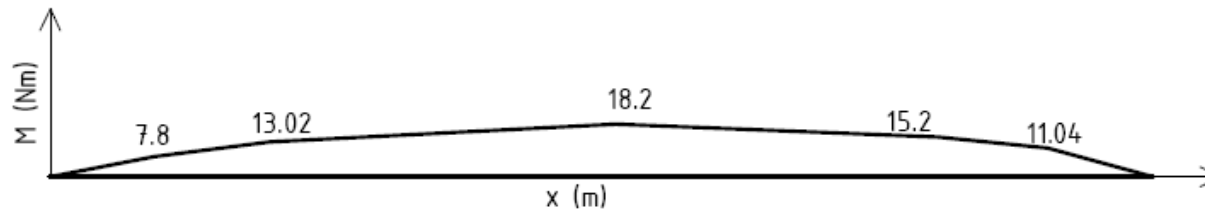


Figure 17. Bending moment diagram

$$M_A = 0$$

$$M_1 = M_A + V_A a_1 = 0 + 65.2 \times 0.12 = 7.8 \text{ Nm}$$

$$M_2 = M_1 + V_1 (a_2 - a_1) = 7.8 + 39.7 (0.2515 - 0.12) = 13.02 \text{ Nm}$$

$$M_3 = M_2 + V_2 (a_3 - a_2) = 13.02 + 13.8 (0.626 - 0.2515) = 18.2 \text{ Nm}$$

$$M_4 = M_3 + V_3 (a_4 - a_3) = 18.2 + -7.6 (1.016 - 0.626) = 15.2 \text{ Nm}$$

$$M_5 = M_4 + V_4 (a_5 - a_4) = 15.2 + -33 (1.142 - 1.016) = 11.04 \text{ Nm}$$

$$M_B = M_5 + V_5 (L - a_5) = 11.04 + -92 (1.262 - 1.142) = 0 \text{ Nm}$$

To size the bolts at C, the shear force at C from the shear force diagram is used. It can be seen that the shear force at C is equal to $V_2 = 13.8 \text{ N}$

The two bolts are under single shear, therefore the shear stress in the bolt become:

$$\frac{\sigma_y}{n} = \frac{V_2}{A}$$

Where n is the factor of safety and A is the cross-sectional area of the pin.

Expressing the area in terms of the diameter: $A = \frac{\pi d^2}{4}$, substituting in () and make “d” the

subject of the formula:

$$\begin{aligned}d &= \sqrt{\frac{4nR_B}{\pi\sigma_y}} \\&= \sqrt{\frac{4 \times 4 \times 13.8}{\pi \times 340 \times 10^6}} \\&= 4.5 \times 10^{-4} \text{ m} \\&= 0.45 \text{ mm}\end{aligned}$$

Again the forces are negligible and don't dictate the design; 6 mm bolts were selected.

From the bending moment diagram, the maximum bending moments in the rods and in the plates are 15.2 and 18.2 Nm respectively. To determine if the axle can resist these bending moments, the required section modulus to resist these bending moments will be calculated and compared to the section modulus of the shaft at those positions. If the required section modulus is less than the section modulus at that position the shaft dimensions are ok and if it is the reverse, the shaft shall be sized to the calculated section modulus.

For the rods:

$$\begin{aligned} S_{\text{req}} &= \frac{nM_{\text{max}}}{\sigma_y} & (18) \\ &= \frac{4 \times 15.2}{340 \times 10^6} \\ &= 1.79 \times 10^{-7} \text{ m}^3 \end{aligned}$$

$$\begin{aligned} S &= \frac{\pi d^3}{32} & (19) \\ &= \frac{\pi 0.025^3}{32} \\ &= 1.5 \times 10^{-6} \text{ m}^3 \end{aligned}$$

For the plates:

$$\begin{aligned} S_{\text{req}} &= \frac{nM_{\text{max}}}{\sigma_y} \\ &= \frac{4 \times 18.2}{340 \times 10^6} \\ &= 2.14 \times 10^{-7} \text{ m}^3 \end{aligned}$$

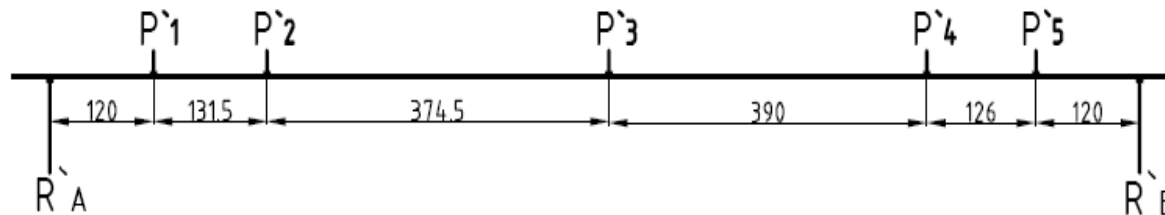
$$S = \frac{bh^2}{6} \quad (20)$$

$$= \frac{0.006 \times 0.04^2}{6}$$

$$= 1.6 \times 10^{-6} \text{ m}^3$$

Since the required section moduli are less than the section moduli at points of maximum bending moments, the proposed dimensions are capable of carrying the loads.

Figure 15 is again shown here for reference for calculating the shaft deflection.



To determine the shaft deflection, the method of superposition shall be employed. Consider the FBD of the shaft in the inclined plane with P_1 acting alone:

E = 200 GPa

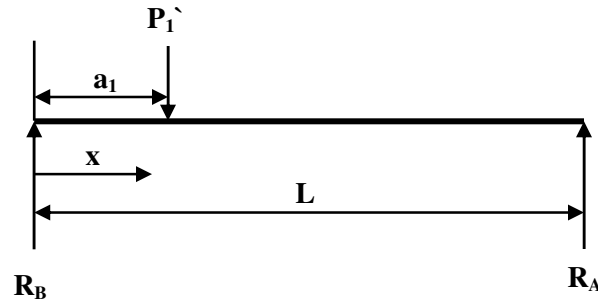


Figure 18. Free body diagram of shaft with $P1\hat{}$ acting alone, superposition

According to Gere, the equations of deflection curves of a simply supported beam (which is the equivalent of the shaft in this case) subjected to one point load on both sides of the load is given by:

$$y = -\frac{P(L - a_n)x}{6LEI_x}(L^2 - (L - a_n)^2 - x^2) \quad 0 \leq x \leq a_n \quad (21)$$

$$y = -\frac{P(L - a_n)x}{6LEI_x}(L^2 - (L - a_n)^2 - x^2) - \frac{P(x - a)^3}{6EI} \quad a_n \leq x \leq L \quad (22)$$

Since the axel is non-prismatic, the flexural rigidity EI is not constant, therefore subscript x in front of I denotes that the second moment of area is changing with x.

For example for P_1 acting alone, the above two equations are used as follow:

For the section A1:

$$y = -\frac{P(L - a_n)x}{6LEI_{A1}}(L^2 - (L - a_n)^2 - x^2)$$

For the section 1C:

$$y = -\frac{P(L - a_n)x}{6LEI_{1C}}(L^2 - (L - a_n)^2 - x^2) - \frac{P(x - a)^3}{6EI_{1C}}$$

For the section CD:

$$y = -\frac{P(L - a_n)x}{6LEI_{CD}}(L^2 - (L - a_n)^2 - x^2) - \frac{P(x - a)^3}{6EI_{CD}}$$

For the section DB:

$$y = -\frac{P(L - a_n)x}{6LEI_{DB}}(L^2 - (L - a_n)^2 - x^2) - \frac{P(x - a)^3}{6EI_{DB}}$$

$$y_{\max} = 0.00079 \text{ mm}$$

Doing the same for all loads, these equations were used in the excel spreadsheet and the deflection curves for individual loads as well as the total deflection curve were plotted as shown below.

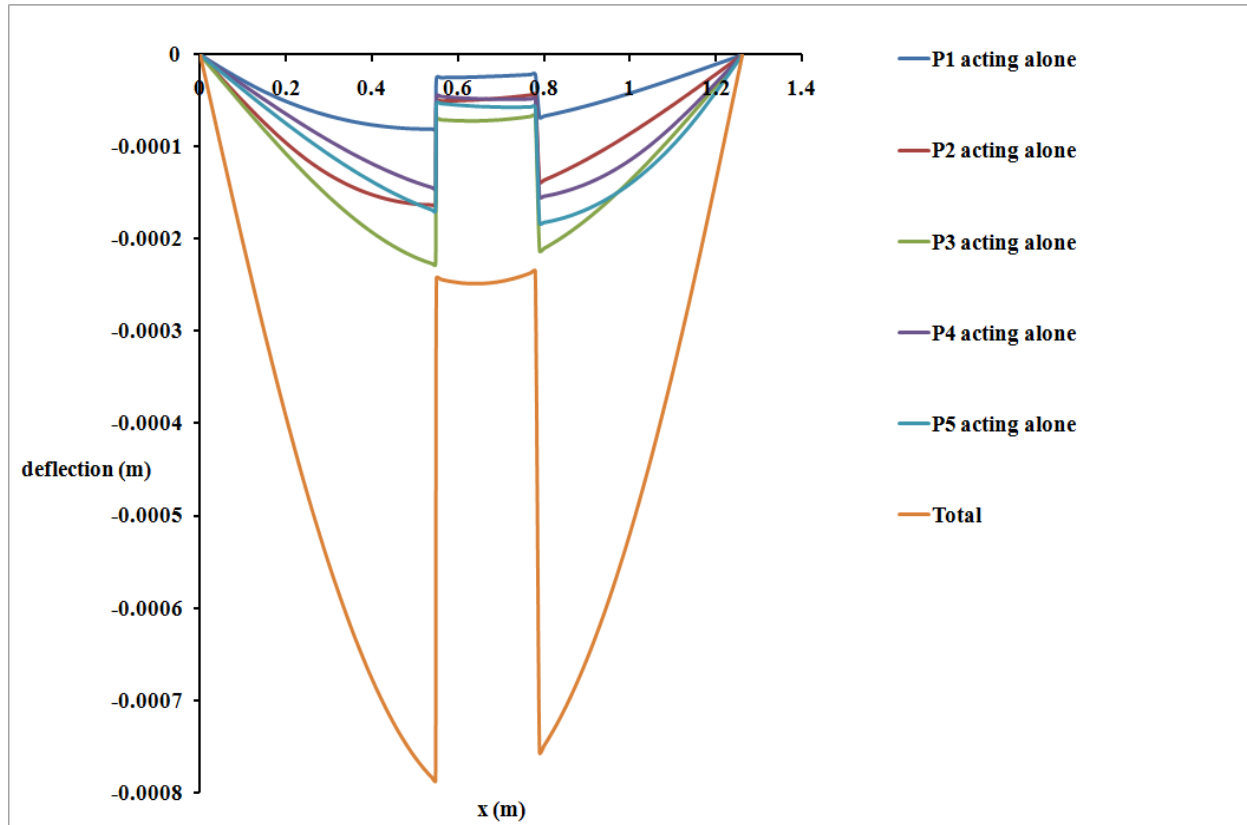
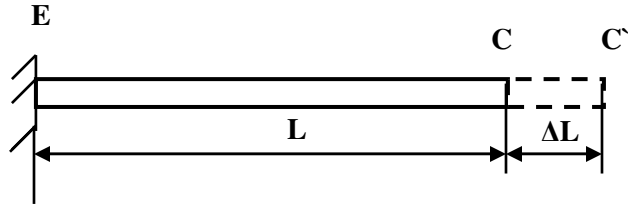


Figure 19. Shaft deflection curves

Even the shaft deflections due to forces applied are very small, maximum 0.00079 mm as can be seen on

	<p>figure 13. The deflection at the middle of the shaft is small compared to what it would have been if the shaft were made from circular rods only. This is because the rectangular plates at the middle have a high second moment of area.</p>	
--	--	--

c) Thermal effects

Initial data	Calculations and sketches	Results
<p>L = 209 mm $\Delta T = 100^\circ\text{C}$ $\alpha = 11 \times 10^{-6}$</p>	<p>At the focal point, the shaft will be subjected to a high temperature of about 120°C and this will cause the shaft to elongate to some extent. The shaft component subjected to this temperature is member CE (see figure 11), which is 6×20 mm 0.209 m long flat steel bar (see drawing 11 Of 25, details L). Consider the free body diagram of this member separated from AC and EB.</p> <div style="text-align: center;">  </div> <p><i>Figure 20. Member CE under thermal expansion</i></p> <p>The change in length of the bar is given by:</p> $\Delta L = L\alpha\Delta T \tag{23}$ <p>Where: L – bar length</p>	<p>$\Delta L = 0.23$ mm</p>

α – coefficient of linear expansion of steel

ΔT – change in temperature

ΔL – bar change in length

Therefore the change in length is:

$$\begin{aligned}\Delta L &= 0.209 \times 11 \times 10^{-6} \times 100 \\ &= 0.0002299 \text{ m} \\ &= 0.2299 \text{ mm}\end{aligned}$$

The change in length of the bar is very small, less than half a millimeter. The clearance at the shaft pin supports (at A and B on figure 11) will provide for this change in length so that no compressive stresses are set up in the shaft, shear stresses in pins and bearing stresses on supporting brackets/columns.

d) Bearing selection

Forces can be neglected in this design as indicated in the above calculations, as results bearings were chosen just to fit on the shaft and no calculations were done. The following bearings were selected from the catalogue:

- Bottom bearing: TR UCFL205
- Top bearing: TR UCFL204

e) Actuator mounting frame

The actuator is mounted on the frame made from 19×19×2 mm rectangular columns and brackets made from 25×25×3 mm angle iron. It is shown in figure 21.

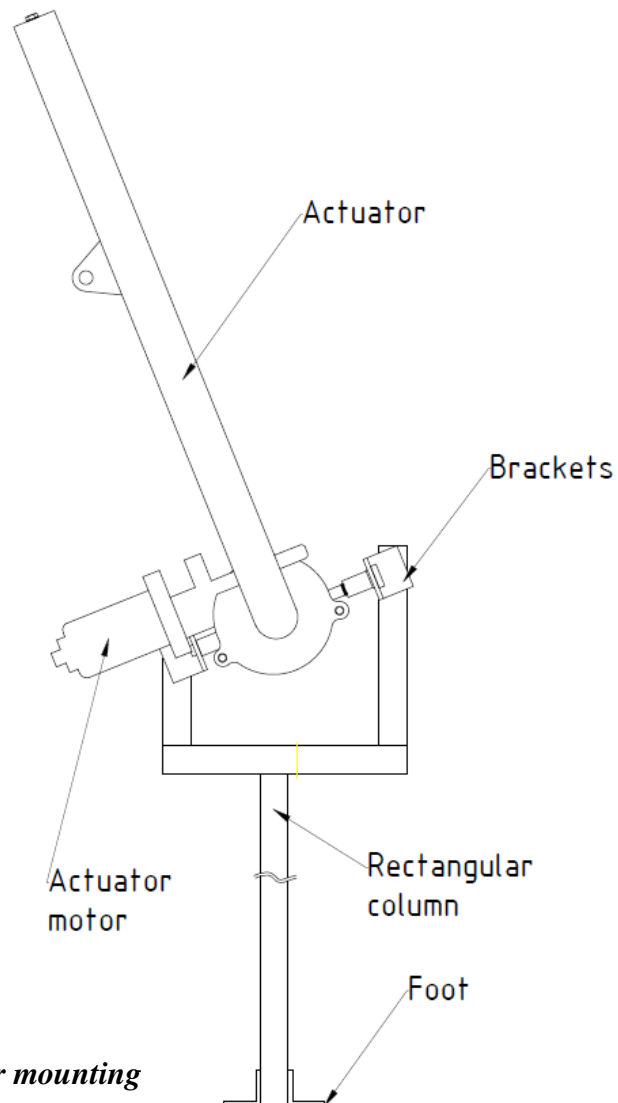


Figure 21. Actuator mounting

7. Manufacturing methods

The manufacturing process consists of cutting, cylindrical turning, milling, tapping, bending, rolling, drilling and arc welding and soldering.

Cutting

Plates and rectangular tubes were cut to size with a sawing machine, guillotine and/or grinder.

Cylindrical turning

Stepped rods that made up the shaft were turned on the lathe machine. All cylindrical components e.g. pins were also manufactured on the lathe.

Milling

Flat surfaces on cylindrical components like shaft rods, thrust collar were milled on the milling machine.

Tapping

Threaded holes and rods were cut with taps and dies.

Bending

The sensor mounting bracket was bend on the bending machine.

Rolling

The round actuator cover was rolled with a rolling machine.

Drilling

All holes on components were made by drilling.

Arc welding and soldering

All permanent joints on the frames were arc welded with either butt or fillet welds. Galvanized sheets e.g. screw cover and electrical components were soldered.

8. Assembly of components

8.1 Parabolic dish

The parabolic dish is bolted to mounting plates which in turn has flange bearings bolted onto them. These bearings sit on the shaft. The shaft is pinned on $32 \times 32 \times 2$ mm steel column which are further bolted on the frame made from the same steel and dimensions. The frame was done in the first phase of the project it was just modified to fit this application:

- Its height was reduced from 1200 mm to 600 mm to be accessible during use.
- Holes were drilled onto it to be able to fit on the dish and actuator columns.

The dish moment arm is fixed on the top plate and the actuator force will be transmitted to the dish through the moment arm. A section through the parabolic dish assembly (excluding the frame) is shown in figure 22.

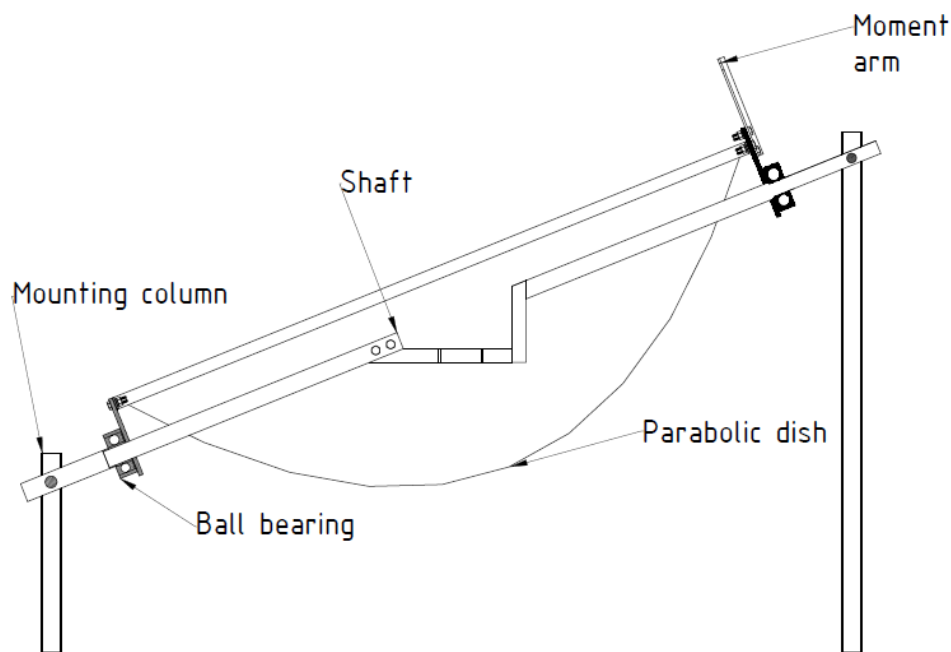


Figure 22. A section through the dish assembly

8.2 Actuator

The actuator is made up of motor, lead screw and the thrust collar. The motor drive shaft is slide-fitted in the lead screw hub and locked in place with two hexagonal cap screws. The thrust collar is threaded on the lead screw and it moves up and down freely when the motor is rotated. The collar connects the

actuator to the dish moment arm. To prevent dust falling on the screw threads, the screw is covered with a tube-like guard. This guard also acts as a safety guard covering rotating components. A section through the actuator is shown in figure 23 below.

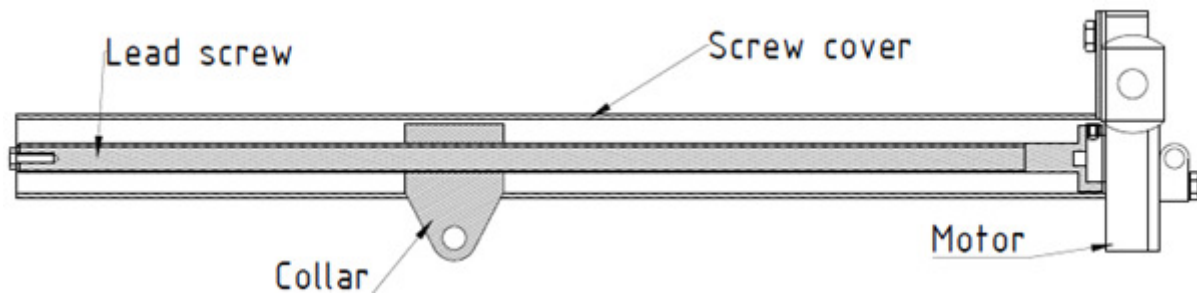


Figure 23. A section through the actuator

8.3 Solar panel

The solar panel is also fixed on the top plate, aligned parallel to the shaft axis and together with the dish they rotate as an integral unity. The sensor is mounted on the high end of the solar panel to prevent it from any shading. The controller is bolted in the corner on the frame as shown in figure 24 to protect it from damage.

Finally, the actuator and the dish are connected together at by the coupling pin and together with the frame; the front view assembly of all parts is shown below.

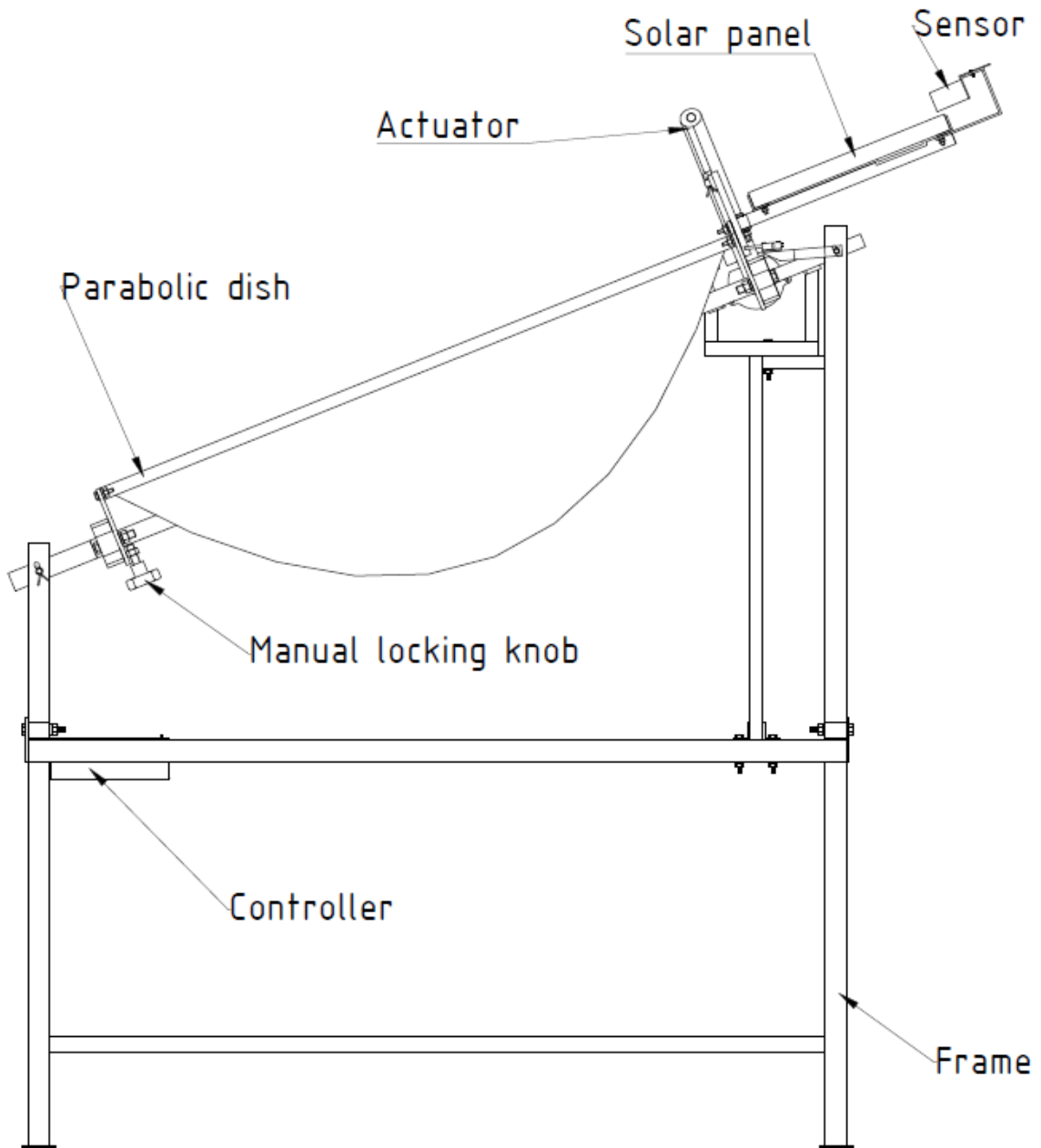


Figure 24. Front view of all parts assembled together

8.4 Painting

To avoid corrosion, supporting frames were painted white while the shaft painted black because black enhance heat absorption.

9. Safety

During use of this parabolic dish, the following safety measures must be taken into considerations:

- The system must be switched off during maintenance of any kind.
- A user must not put his/her hand on the absorber platform (focal point) during operation because it gets too hot and severe burns may occur.
- A user must not look directly at the focal point with naked eyes when there is nothing on the absorber platform because the dish material is highly reflective and this may damage eyes.
- The parabolic dish must not be used on automatic mode unless the actuator cover/guard is in place.
- No person must be under the dish or solar panel for shade or whatever purpose during use as this may cause injuries when the dish moves.

10. Testing and results

After assembling all components together, the system was tested.

1. While the system is off, the dish was sufficiently kept away from the sun and switched on to see if it will seek and orient itself facing the sun. As expected, as soon as it is switched on, the controller switches on the motor to rotate the dish to face where the sun is. Figure 25 shows some pictures taken during testing on the roof of the engineering building. The roof top was chosen as a testing place because there no is shading.



Figure 25. Tracking system being tested

2. Another test done was shading one side of the sensor while the dish is facing the sun to simulate the effect when the sun moves and remove the shading after some time. Once one side is shaded, the controller switches on the actuator to correct the dish position. When the shading is removed, the actuator brings the dish to its original correct position before shading.
3. The dish was left in the sun for the whole day and just inspected at one hour interval. Every time it was found facing the sun.

4. Finally the dish was used to cook macaroni. Although the objective of this project was to design the tracking system, cooking was just done to see if it will really cook something. It took approximately 60 minutes to cook.

During testing, the actuator performance was also observed. The actuator was rotating the dish with easy even at small transmission angles, the actuator has no difficulties in tilting the dish. This was not surprising because the torque required to rotate the dish was found (see section 6.3.1 (c)) to be less than 70 % of the motor torque.

11. Cost analysis

The cost analysis was done based on the bill of material used in the project.

Table 3. Bill of Material

Material or part	Quantity	Cost (NAD)	
12 V DC motor	1	300.00	
Solar tracker controller including: sensors, cables, battery, solar panel	1	2000.00	
Limit switch	1	29.40	
On/Off switch	1	10.50	
Cables ties	10	5.00	
Parabolic dish	1	1800	
3 mm flat plate	24696 mm ²	This items were not bought for this project, they were provided in the workshop, however they are estimated to cost N\$1500	
6 mm flat plate	40425 mm ²		
25 mm diameter steel rod	800 mm		
32 mm diameter steel rod	800 mm		
420 mm Lead screw with P = 1.5 and d =14 mm	1		
25×25×3 mm Angle iron	860 mm		
19×19×2 mm rectangular tube	1700 mm		
25×50×2 mm rectangular tube	1936 mm		
32×32×2 mm rectangular tube	6520 mm		
1 mm galvanized sheet	14400 mm ²		
M10 x50 mm Bolts, nuts and washers	4		60.60
M8 x50 mm bolts and nuts	5		
M6 x 50 mm bolts and nuts	3		
M6 x 40 mm bolts	2		
M6 x 20 mm bolt and nuts	6		

M6 x 15 mm bolt	1	
M6 x 10 mm bolt	1	
M5x15 mm bolts and nuts	4	
M4 x 15mm bolts	3	
M4 hexagonal set screws with coned end	2	
M3 bolt and nut	1	
6 mm external circlip	1	
10 mm external circlip	1	
3.5 mm split pins	2	
Ball bearing: TR UCFL205	1	61.12
Ball bearing: TR UCFL204	1	50.62
Heat resistant black paint, Deluxe	300 ml	59.95
White paint, Enamel	1L	75.45
Total cost		N\$ 5952.64

The total cost of commercial solar tracking system for similar application will be around 8000 NAD. It is seen that the developed system is cost effective.

There are two customers who will buy the solar dish with tracking system : rural area customer and an urban area customer:

11.1 Rural area customer

If this person buys the solar dish cooker, it will save him time that he used to look for firewood and use this time in some other productive ways. It will also benefit the environment because deforestation will be reduced. In this case the customer has invested into living comfortably and makes his life easier.

The customer won't get the reward in monetary terms but on the time saved and other benefits mentioned above.

11.2 Urban area customer

If this customer buys the dish cooker, it will save him money he spends on electricity for cooking. The payback time is less than one year maximum for households depending on how much food is cooked per day. After this one year onward, cooking will be free.

Even in urban areas, the dish cooker has environmental advantage: the power demand on the power utility generators will be reduced, which means less fuel is burned.

12. Conclusions and recommendations

In this project, the automatic sun tracking system was designed, incorporated on the parabolic dish cooker and tested and it works as expected. To be honest, there was no fear that the system might not work because the sun tracking controller was bought from the company that specializes in sun tracking designs. A project has been given to an electrical engineering student to design a controller and use it on the hardware manufactured in this project. The main challenge in this project was to incorporate this technology on the parabolic dish, the actuator design (especially motor selection) and the absorber platform.

The actuator is also working as expected but it is shaking a little bit and this induces some vibration on the system. Vibration absorbers may be used on the actuator mountings e.g. rubber mountings.

Since the automatic sun tracking system works on the parabolic dish, this encourages further research in the project for improvements so that the refined product can be used in rural areas of Namibia.

Appendix (drawings)

Enclosed

Bibliography

1. The Ecliptic: the Sun's Annual Path on the Celestial Sphere. <http://E:\Project\downloads\Solar Year.htm>
2. S. Wieder. 1992. An Introduction to Solar Energy for Scientists and Engineers. John Wiley & Sons Inc. USA
3. W. J. Kaufmann. 1991. Universe. Third edition. W. H. Freeman and Company. New York.
4. T. Amupadhi. (2010). A ray of hope. Insight Namibia. April 2010. pp. 28
5. Germany Solar Energy Society (DGS). 2005. Planning and installing photovoltaic systems: a guide for installers, architects and engineers. James & James science publisher. UK
6. http://en.wikipedia.org/wiki/Passive_daylighting: (1 April 2010)
7. The Rex Research Civilization Kit. (18 May 2010) Solar Furnace / Concentrator Patents. <http://www.rexresearch.com/solrfurn/solfrnpat.htm>
8. Personal communication Mr. Conrad Roedern (Electronic engineer). Managing Director & Founder of Solar Age Namibia (PTY) LTD. March 2010
9. Personal communication. Mr. Heinrich Steuber (Mechanical engineer). Director at Soltec cc 7 April 2010
10. Air University Islamabad. (1 April 2010). Automatic Sun Tracking System. www.handasarabia.org/mambo/index.php?option=com
11. P. Roth. A. Georgiev. H. Boudinov. Technical note, Design and construction of a system for sun-tracking. (1 April 2010) <http://placeres.mec.utfsm.cl/www.labsolar.utfsm.cl/images/stories/media/ageorgiev5.pdf>.
12. Research report on *PARABOLIC DISH SOLAR WATER HETER*